



Reprint 2018-3

The Impact of Water Scarcity on Food, Bioenergy and Deforestation

N. Winchester, K. Ledvina, K. Strzepek and J.M. Reilly

Reprinted with permission from *Australian Journal of Agricultural and Resource Economics*, online first (doi:10.1111/1467-8489.12257).

© 2018 the authors

The MIT Joint Program on the Science and Policy of Global Change combines cutting-edge scientific research with independent policy analysis to provide a solid foundation for the public and private decisions needed to mitigate and adapt to unavoidable global environmental changes. Being data-driven, the Joint Program uses extensive Earth system and economic data and models to produce quantitative analysis and predictions of the risks of climate change and the challenges of limiting human influence on the environment—essential knowledge for the international dialogue toward a global response to climate change.

To this end, the Joint Program brings together an interdisciplinary group from two established MIT research centers: the Center for Global Change Science (CGCS) and the Center for Energy and Environmental Policy Research (CEEPR). These two centers—along with collaborators from the Marine Biology Laboratory (MBL) at

Woods Hole and short- and long-term visitors—provide the united vision needed to solve global challenges.

At the heart of much of the program's work lies MIT's Integrated Global System Model. Through this integrated model, the program seeks to discover new interactions among natural and human climate system components; objectively assess uncertainty in economic and climate projections; critically and quantitatively analyze environmental management and policy proposals; understand complex connections among the many forces that will shape our future; and improve methods to model, monitor and verify greenhouse gas emissions and climatic impacts.

This reprint is intended to communicate research results and improve public understanding of global environment and energy challenges, thereby contributing to informed debate about climate change and the economic and social implications of policy alternatives.

—*Ronald G. Prinn and John M. Reilly,*
Joint Program Co-Directors

The impact of water scarcity on food, bioenergy and deforestation*

Niven Winchester, Kirby Ledvina, Kenneth Strzepek and
John M. Reilly[†]

We evaluate the impact of explicitly representing irrigated land and water scarcity in an economy-wide model with and without a global carbon policy. The analysis develops supply functions of irrigable land from a water resource model for 282 river basins and applies them within a global economy-wide model. The analysis reveals two key findings. First, explicitly representing irrigated land has a small impact on global food, bioenergy and deforestation outcomes. This is because this modification allows irrigated and rainfed land to expand in different proportions, which counters the effect of rising marginal costs for the expansion of irrigated land. Second, changes in water availability have small impacts on global food prices, bioenergy production, land use change and the overall economy, even with large-scale (*c.* 150 exajoules) bioenergy production, due in part to endogenous irrigation and storage responses. However, representing water scarcity and changes in water availability can be important regionally, with relatively arid areas and/or areas with rapidly growing populations fully exhausting our estimated maximum irrigation capacity that allows for improved irrigation efficiency, lining of canals to limit water loss, and expanding storage to fully capture average annual water flows.

Key words: bioenergy, climate change, food, irrigation, water.

1. Introduction

In future decades, economic growth and rising population will drive increased food demand. At the same time, energy and climate policies may promote the production of bioenergy creating a new competitor for land resources. Given

* The authors wish to thank Rosemary Albinson, Bo Chen, Andrew Cockerill, Jo Howes, Fabio Montemurro, James Primrose and Cameron Rennie for helpful comments and suggestions. Primary funding for this research was through a sponsored research agreement with BP. The authors also acknowledge support in the basic development of the Economic Projection and Policy Analysis model from the Joint Program on the Science and Policy of Global Change, which is funded by a consortium of industrial sponsors and Federal grants. For a complete list of sponsors see for complete list see <http://globalchange.mit.edu/sponsors/current.html>). The findings in this study are solely the observations of the authors.

[†] Niven Winchester (email: niven@mit.edu) is Principal Research Scientist, Kirby Ledvina is Research Associate with Joint Program on the Science and Policy of Global Change, Massachusetts Institute of Technology, 77 Massachusetts Avenue, E19-439h, Cambridge, Massachusetts, USA. Kenneth Strzepek is a Research Scientist in Joint Program on the Science and Policy of Global Change, Massachusetts Institute of Technology and Professor Emeritus of Civil, Environmental, and Architectural Engineering, University of Boulder at Colorado. John M. Reilly is Co-Director in Joint Program on the Science and Policy of Global Change, Massachusetts Institute of Technology and Senior Lecturer at the MIT Sloan School of Management.

demand growth for conventional agricultural products, and exogenous trends in productivity of agricultural production, the basic margins of adjustment that will determine if there is ‘room’ for biomass energy expansion include: (i) whether yields on existing cropland can increase in response to land price increases (intensification); (ii) whether cropland area can expand (extensification); and (iii) whether food usage can decrease in response to higher food prices. In general, with a new demand for land, we would expect movement on all three margins, but how much on each depends on how fast costs rise on each margin as expansion advances.

A key intensification option is to irrigate more land already in agricultural production, as yields on irrigated land are typically far above those on rainfed land. The feasibility of expanding irrigated production will depend on the costs of investments in irrigation infrastructure. Moreover, expanding the extensive margin raises concerns about the destruction of natural habitat, deforestation and carbon storage.

Water resource limits and policies regarding protection of natural lands could put more pressure on the food demand response margin, potentially pricing the lowest-income populations out of the food market. Rising greenhouse gas (GHG) concentrations and the associated changes in climate – which will largely depend on future energy production and land use – will also impact food and water systems. Food, energy, water and land use outcomes, therefore, must be considered as an interconnected system.

This paper quantifies tradeoffs among these margins and bioenergy potential by improving the representation of irrigation potential in the MIT Economic Projection and Policy Analysis (EPPA) model (Paltsev *et al.* 2005), a global model linking economic activity, natural resources, land use change and GHG emissions. Specifically, we represent irrigable land supply curves, estimated from detailed spatial data on water availability and irrigation costs, in the EPPA model. A global carbon price is simulated in the model under alternative water availability assumptions to estimate how constraints on the expansion of irrigated land, as represented by irrigable land supply curves, will impact food prices, bioenergy production and deforestation.

Several previous studies have used economy-wide models to examine water issues – see Dinar (2014) for a review of this literature. The most relevant strand of previous research for this analysis examines the impacts of water constraints on food and other outcomes using the GTAP-BIO-W model (Taheripour *et al.* 2013a).¹ This model represents irrigated and rainfed crop production at the agro-ecological zone (AEZ) level and divides the water system into 126 river basins. Rainfed and irrigated crop production compete for land at the river basin-AEZ level, and there is competition for water resources at the river basin level.

¹ Earlier work on representing water for agriculture in economy-wide models includes Berrittella *et al.* (2007) and Calzadilla *et al.* (2010).

Taheripour *et al.* (2013b) examine alternative constraints on the expansion of irrigated land and conclude that studies that fail to distinguish rainfed and irrigated land underestimate global land use change and emissions induced by the expansion of corn ethanol production in the US. Liu *et al.* (2014) use the GTAP-BIO-W model to simulate the impact of changes in water available for irrigation estimated by Rosegrant *et al.* (2012). Due to significant declines in projected water availability in key river basins, the authors estimate significant decreases in agricultural production in China, South Asia and the Middle East. However, global impacts are modest as agricultural trade buffers heterogeneous regional impacts.

While the GTAP-BIO-W model has advanced economy-wide modelling of food, water and bioenergy outcomes, at least two limitations remain. First, the model assumes that the supply of accessible land is fixed, so while there is land conversion among forestry, pasture and cropland, it does not consider deforestation due to the conversion of (currently) inaccessible land to managed uses. Second, the model does not currently allow investment in irrigation systems and/or water storage in response to changes in relative prices, which could be driven by water scarcity or rising food demand.

We apply a framework that addresses these limitations in four further sections. Section 2 provides an overview of our economy-wide model and the estimation of irrigable land supply curves. Section 3 outlines scenarios considered in our modelling analysis. Section 4 presents and discusses results. Section 5 offers concluding remarks.

2. A global model of the economy, energy, and agriculture

Our analysis builds on the EPPA model with land use (Gurgel *et al.* 2007, 2011), a global model of economic activity, energy production and GHG emissions. We start with a version of the EPPA model augmented to consider land use change and bioenergy in detail (Winchester and Reilly 2015) and extend it to represent rainfed and irrigated land and the costs and limitations of expanding irrigated areas.

2.1 The Economic Projection and Policy Analysis model

The EPPA model is recursive-dynamic, multiregion computable general equilibrium global model and is solved through time in 5-year increments from 2005 through 2050. Regions and sectors represented in the model are outlined in Table S1. For each of the 16 countries or regions in the model, 14 broad production sectors are defined: five energy-producing sectors (coal, crude oil, refined oil, gas and electricity), three agricultural sectors (crops, livestock and forestry), and six other nonenergy sectors (energy-intensive industry, commercial transportation, private transportation, food products, services and other industries). Several commodities in the model can be produced using different technologies and/or resources, including 'advanced

technologies'. For example, refined oil products can be produced both from crude oil and biofuels. Due to their higher costs, advanced technologies typically do not operate in the base year but may become cost competitive due to changes in relative prices caused by policies or resource depletion. Fossil fuel prices are endogenously estimated, a result of demand for fuels in the economy interacting with the specification of resource availability and supply technology. The oil price rises through time and reaches \$123.90 per barrel by 2050 in 2010 dollars. While energy prices are notoriously variable this forecast is in line with other sources such as projections by the IEA (2012).

Following Winchester and Reilly (2015), the model used for this analysis includes (i) seven first-generation biofuel crops and conversion technologies; (ii) a representative energy grass and a representative woody crop; (iii) agricultural and forestry residues; (iv) lignocellulosic (LC) ethanol via a biochemical process and LC drop-in fuel using a thermochemical process; (v) an ethanol-to-diesel upgrading process; (vi) electricity from biomass and (vii) heat from biomass for use in industrial sectors. The model also explicitly represents bioenergy co-products (e.g. distillers' dry grains), international trade in biofuels, and limits on the blending of ethanol with gasoline. Whether some, all, or none of these technologies will operate in the future depends on the basic input requirements specified for each technology, the prices of these inputs as endogenously determined and varied over time, and the output price when compared against the reference fuel with which it competes. For this analysis, we update the LC ethanol costs in Winchester and Reilly (2015) to reflect estimates by BP (2015). Under these projections, the cost of LC ethanol, in 2010 dollars per gasoline equivalent gallon, falls through time and from \$7.10 in 2015 to \$2.63 in 2050.

Production sectors are represented by nested constant elasticity of substitution (CES) production functions. Inputs for each sector include primary factors (labour, capital, land and energy resources) and intermediate inputs. For climate policy analysis, important substitution possibilities include the ability for producers to substitute among primary energy commodities, and between aggregate energy and other inputs. Goods are traded internationally and differentiated by region of origin following the Armington assumption (Armington 1969), except for crude oil and biofuels, which are homogenous goods.

Factors of production include capital, labour, resources specific to energy extraction and production, and six land types (cropland, managed forest land, natural forest land, managed grassland, natural grassland and other land). In this version of the model land use change is represented following Gurgel *et al.* (2007) and Melillo *et al.* (2009). The approach explicitly represents conversion costs by requiring inputs of capital, labour and intermediate inputs in the transformation process, and consistency in land accounting is maintained by combining land and other inputs in a Leontief nest (i.e. 1 ha of one land type is required to produce 1 ha of another land

type). If land is being converted from natural forests, in addition to 1 ha of another land type, there is a one-time output of timber associated with clearing the land.

The responsiveness of land conversion of natural forestland or natural grassland to a managed land type in each region is parameterized as an elasticity of land supply estimated to represent historical relationships between changes in land use and land rents. As noted by Gurgel *et al.* (2007, p. 15), ‘underlying this response may be increasing costs associated with specialised inputs, timing issues in terms of creating access to ever more remote areas, and possible resistance to conversion for environmental and conservation reasons that may be reflected in institutional requirements and permitting before conservation’. Increased land rents cause small changes in deforestation in developed regions, while deforestation is most sensitive to changes in land rents in Africa and Other Latin America (Gurgel *et al.* 2007).

There is a single representative utility-maximising agent in each region that owns all factor endowments in the region, derives income from factor payments and allocates expenditure across goods and investment. A government sector collects revenue from taxes and (if applicable) emissions permits, and purchases goods and services. Government deficits and surpluses are passed to consumers as lump-sum transfers. Final demand separately identifies household transportation and other commodities purchased by households. Household transportation is comprised of private transportation (purchases of vehicles and associated goods and services needed to run and maintain them) and purchases of commercial transportation (e.g. transport by buses, taxis and airplanes). The model projects emissions of GHGs (carbon dioxide (CO₂), methane, nitrous oxide, perfluorocarbons, hydrofluorocarbons and sulfur hexafluoride) and conventional pollutants that also impact climate (sulfur dioxide, carbon monoxide, nitrogen oxide, nonmethane volatile organic compounds, ammonia, black carbon and organic carbon).

The model is calibrated using economic data from Version 7 of the Global Trade Analysis Project (GTAP) database (Narayanan and Walmsley 2008),² population forecasts from the United Nations Population Division (UN 2011), and energy data from the International Energy Agency (IEA 2006, 2012). Regional economic growth through 2015 is calibrated to International Monetary Fund (IMF) data (IMF 2013). The model is coded using the general algebraic modelling system (GAMS) and the Mathematical Programming System for General Equilibrium analysis modelling language (Rutherford 1995).

2.2 Representing irrigated land in the EPPA model

As noted in Section 2.1, the EPPA model includes a single, aggregated cropland type. We extend the model by explicitly representing rainfed and

² See Aguiar *et al.* (2016) for an overview of the most recent version of GTAP database.

irrigated areas, and the scope for expanding irrigated land. There are three necessary steps: (i) disaggregate cropland and production into irrigated and rainfed components; (ii) calibrate multiple irrigable land supply curves for each EPPA region that describe how the marginal cost of irrigated land increases with expansion to capture the within-region variability in crop yields and water availability³; and (iii) augment the EPPA model to represent irrigated and rainfed crop production and, irrigable land supply curves. In the extended EPPA model, we assume bioenergy crops are only grown on rainfed land, which is consistent with assumptions used to estimate yields for bioenergy feedstocks and prevailing practices; however, the indirect effect of using more rainfed land for energy crops may be to increase irrigation of other crops to increase their yields.

2.2.1 Production on irrigated and rainfed areas

We first identify current rainfed and irrigated areas and the value of production on those land types. To disaggregate cropland in the EPPA model, we use data on harvested area for rainfed and irrigated areas from the monthly irrigated and rainfed crop areas (MIRCA2000) data set (Portmann *et al.* 2010). These data are available at a spatial resolution of 5 arc-minutes by 5 arc-minutes (about 10 km by 10 km) for 26 crop types. We aggregate the data spatially and across crop types to calculate total rainfed and irrigated areas for each grid cell. Figure S1 presents irrigated and rainfed land for each EPPA region. At the global level, 76.1 per cent of cropland is rainfed and 23.9 per cent is irrigated. The portion of irrigated land in total harvested area is largest in the Middle East, China, Japan, the Rest of East Asia and India. Conversely, the fraction of cropland that is irrigated is relatively low in Australia-New Zealand, Europe, Africa, Brazil, Russia and Canada.

The value of production on each land type in each region is estimated by combining the MIRCA2000 harvested area data with price and yield data. Crop prices in 2000 by country are sourced from the Food and Agricultural Organization (FAO) and yield data are taken from Siebert and Döll (2010). These data, like the harvested area data, are available at a spatial resolution of 5 arc-minutes by 5 arc-minutes for 26 crop types. Consequently, we calculate production by crop and land type at this level of aggregation using appropriate country-level prices for each grid cell. To match the 26 (aggregate) crop types, we calculate production-weighted average prices. For example, the price for citrus from the MIRCA data set is computed using a combination of the FAO prices for grapefruit, lemons, limes, oranges and other citrus fruits. For presentation purposes, the value of crop production on each land type is aggregated to EPPA regions, as shown in Figure S2. The

³ Sections 2.2.1 and 2.2.2 provide an overview of the approach used for, respectively, steps (i) and (ii). A companion paper, Ledvina *et al.* (2017), presents a detailed description of the methods used to disaggregate crop land and estimate of irrigable land supply curves. Ledvina *et al.* (2017) also provide supplementary files that allow users to replicate (and modify) the build streams for these activities.

fraction of regional production value from irrigated land is above 50 per cent in the Middle East, India, rest of East Asia, Mexico and China. Conversely, irrigated land is responsible for a relatively low share of production values (<15 per cent) in Brazil, Russia and Canada. Globally, 67.3 per cent of production value comes from rainfed land and 32.7 per cent comes from irrigated land. Given the fractions of rainfed and irrigated land hectares and production value, this implies that on average globally irrigated land is 55 per cent more productive than rainfed land in terms of value of crop produced.

2.2.2 Irrigated land supply curves

The scope for irrigating additional areas relative to the base year is modelled by specifying a suite of supply curves for additional irrigable land. These supply curves allow irrigated areas to be expanded by: (i) improving conveyance efficiency; (ii) improving irrigation efficiency; and (iii) increasing water storage.⁴ The irrigable land supply curves employ the water resource system (WRS) component of the Integrated Global System Model (IGSM; Strzepek *et al.* 2013). The WRS identifies 282 regions referred to as assessment subregions (ASRs) or food producing units (FPUs) by the International Food Policy Research Institute. The ASRs/FPUs are boundaries of the world's major river basins further delineated by national political borders. We group the FPUs into 126 transnational water regions.⁵ Water regions and their constituent FPUs are shown in Figure S3. A list of water regions by EPPA region is displayed in Table S2.

We first develop the irrigable land supply curves at the water region level. In each water region, improving conveyance and/or irrigation efficiency means that the same amount of water can irrigate more land, and an increase in the quantity of water storage increases average water availability. Crop water requirements for each water region from Strzepek *et al.* (2013), which are determined by characteristics such as climate and soil quality, are used to determine how much irrigated land can expand due to improvements in irrigation efficiency and increases in storage.

At a regionally-specific cost, each water region can upgrade its conveyance and irrigation efficiencies from their current levels. Defining conveyance efficiency as the ratio of the amount of water that reaches the field to the amount of water supplied, a canal without lining has a conveyance efficiency of 0.75 and a lined canal has an efficiency of 0.95. Irrigation efficiencies – the ratio of the amount of water consumed by the crop to the amount of water supplied through irrigation – for the four irrigation schemes considered are shown in Table S3. This table also shows overall scheme efficiencies for

⁴ Groundwater does not influence irrigable land supply curves because, in regions suitable for growing crops, groundwater is already allocated to existing activities (maintaining the existing level of irrigated crop production, municipal use etc.) (Strzepek *et al.* 2013).

⁵ The delineation of the 126 water areas in our study matches that in the GTAP-BIO-W model, although we refer these areas as 'water regions' while Haqiqi *et al.* (2016) labels them 'river basins'.

alternative conveyance-irrigation systems, which is the product of conveyance and irrigation efficiencies.

Provided that there is existing irrigation, the least expensive upgrade is always the addition of canal lining to improve conveyance efficiency.⁶ Irrigation efficiency upgrades progress in the order of no irrigation, flood, furrow, low-efficiency sprinkler and high-efficiency sprinkler. For water storage, curves describing the relationship between water storage and water yield (water that is available for consumption each year after accounting for evaporation) are developed following Wiberg and Strzepek (2005) and using estimates from Strzepek *et al.* (2013). In each water region, the water storage-yield curve spans all water storage increases available starting from zero storage. For our purposes, we approximate storage-yield curves using a step function with ten discrete upgrades. Each water region starts at a point of the storage-yield curve consistent with existing storage in that region as estimated by Strzepek *et al.* (2013). Most regions already have some storage and hence most have <10 storage upgrade options to store additional water.

Irrigable land supply curves for each water region are constructed by assembling conveyance and irrigation efficiency and storage options from lowest to highest cost, forming a step function describing supply of additional irrigable land. As the marginal cost of increasing irrigable land by adding additional storage increases, storage upgrades are typically dispersed among conveyance and irrigation efficiency upgrades in each water region. As an example, the supply curve for additional irrigable land in the Mississippi River water region is depicted in Figure S4.

For computational reasons, we aggregate the 126 water region supply curves to a smaller number. As the EPPA model will treat irrigated land within each sub-region as homogenous and it is typically more expensive to expand irrigation in high-yield regions (which have already implemented low-cost irrigation options) than low-yield areas, care must be taken when aggregating water regions. For example, combining irrigable land supply curves for high-yield and low-yield regions would result in yields on newly irrigated land equal to the average for that combination, but at the cost of expanding irrigation in the low-yield region. To avoid this issue, we use *k*-means clustering to group the water regions within each EPPA region with similar rainfed and irrigated yields. We designed the analysis so that each EPPA region contains between one and four clusters of water regions, which we call irrigation response units (IRUs). Figure S5 shows irrigated and rainfed yields for water regions in India, and illustrates the grouping of these

⁶ Based on our interpretation of the initial data, we make a judicious modification to avoid overestimating potential irrigation expansions in rice farming areas in China. Specifically, in the rice paddies, water that leaks out of irrigation pipes prior to its intended destination fell into the rice field, so it is not wasted. Therefore, the benefit of adding lining to the irrigation systems was overestimated in the initial data. We identified those problem regions and decreased irrigable land gains from the lining by 90 per cent in those regions.

regions into three IRUs using different colours. A complete list of IRUs and their constituent water regions is provided in Table S4.

The supply step functions for the water regions within each cluster are aggregated across water regions to form an IRU supply step function. As illustrated in Figure S6, we approximate each IRU step function by estimating a constant elasticity supply function of the form $q = \beta p^\lambda$, where q is the quantity of additional irrigable land, p is the price/cost of irrigating additional hectares, and β and λ are parameters to be estimated. For each ASR and IRU, we also calculate its maximum irrigation potential, which is defined as the area that can be irrigated when annual average water yield is equal to annual average runoff (i.e. all available runoff is stored and used), all irrigation canals are lined, and high-efficiency sprinklers are used for all irrigation.

2.2.3 Representing irrigated and rainfed crop production in the EPPA model

As the GTAP database used to calibrate sectoral production functions in the EPPA model does not differentiate irrigated and rainfed production, irrigation costs are included in payments to factors of production and intermediate inputs in (aggregate) crop production. Our disaggregation approach follows Taheripour *et al.* (2013b) and is applied to each IRU. First, we divide land rental payments net of irrigation costs (innate land payments) between irrigated and rainfed production according to area shares. Second, we allocate the value of aggregate crop production to the two crop production types using production value shares for each IRU. Third, for each production type, we calculate residual production costs as total costs minus land costs and allocate residual costs to other inputs according to each input's cost share in total crop production costs. As irrigated yields are higher than rainfed yields, the value of innate land payments per dollar of irrigated crop production is lower and the value of other inputs higher than that for rainfed production. As a result, irrigation costs in the base year are captured by additional capital and other costs relative to those for rainfed production.

The nested CES production structures for crops produced on irrigated land in each IRU in the EPPA model is sketched in Figure S6. We include an irrigation permit system to ensure that the amount of irrigated land used in each IRU is equal to the amount of available irrigated land in that IRU. Specifically, each hectare of land used in the production of irrigated crops requires an IRU-specific irrigation permit. This is shown in Figure S6 in the Land-irrigation permit nest, where σ_{L-I} equals zero. Initially, each region is endowed with a quantity of irrigation permits equal to the quantity of land currently irrigated in each IRU. Thus, in each IRU, the model allows the current quantity of irrigated land to be maintained by replicating existing costs for irrigated crop production and, as discussed below, it can be expanded at additional costs and subject to water resource constraints. This specification also mandates that adding an additional hectare of irrigated land requires taking 1 ha of land away from rainfed crop production.

The production structure for rainfed crops is identical to that for irrigated crops except that inputs of irrigation permits are not required. Key substitution possibilities in the production functions for both irrigated and rainfed crop production include those between land and the energy materials composite (σ_{L-EM}), and between the resource-intensive bundle and the capital-labour aggregate (σ_{R-KL}). Both of these elasticities allow endogenous yield improvements due to increases in land prices.⁷ Guided by Baker (2011), crops produced in each IRU are imperfect substitutes for each other, and composite irrigated crops are imperfect substitutes for rainfed crops.

Additional irrigation permits can be produced by using water resources and other inputs, as shown in Figure S7, which are added to the original endowment of permits, allowing expansion of irrigation beyond that in the base year data. A key element in this specification is substitution between the capital-labour-intermediates composite and an irrigation specific resource. For each IRU, following the calibration routine outlined by Rutherford (2002), the value of irrigation specific resources and $\sigma_{KLI-ISR}$ is chosen to replicate the elasticities of supply for additional irrigated land estimated in Section 2.2.3. Under this framework, irrigating additional hectares requires not only installing irrigation infrastructure on newly irrigable land, but also upgrading existing infrastructure to free up additional water and/or increasing water storage. The capital, labour and intermediate inputs used in the production of irrigation permits reflect the inputs used to expand irrigable land, thus connecting the expansion with a draw on actual inputs.

As noted above, the supply of irrigable land has a hard upper limit in each IRU; however, the calibrated irrigable land supply curve could allow expansion beyond this limit. To ensure the maximum limits are not exceeded, we introduce another allowance mechanism: irrigation certificates. Each region is endowed with a quantity of IRU-specific irrigation certificates equal to the maximum number of additional hectares that can be irrigated. One certificate is required for each permit that is produced, as shown in the top nest in Figure S7. In our analysis, σ_{KLI-C} equals zero, ensuring that once the endowed number of certificates are exhausted no more irrigation permits can be produced. As long as the limit has not been reached, the shadow value of certificates is zero; once it is reached, there is a positive shadow price on certificates with rents going to the representative household in the region. The model assumes that new cropland has the same productivity as existing cropland in each EPPA region (for rainfed cropland) and in each irrigation response unit (for irrigated cropland).

These assumptions are supported by findings from Taheripour *et al.* (2012). Using a highly resolved terrestrial ecosystem model, they show that

⁷ Previous versions of the EPPA model have implicitly considered the expansion of irrigated areas through substitution between resource-intensive and capital-labor bundles. This option is now explicitly modeled, so we decrease the value of set σ_{R-KL} from 0.7 used in previous versions to 0.55.

currently unused land in a particular region has similar innate productivity to existing cropland. As noted in van Tongeren *et al.* (2017, p. 26) possible reasons for this include: (i) factors such as road access are more important than productivity in determining land use; and (ii) innate characteristics of the land may have relatively little to do with its productivity as cropland, rather it is mostly determined by investments in the land.

3. Scenarios

To address the question posed in the introduction, we consider eight scenarios that differ with respect to: (i) policies; (ii) whether or not irrigated land is explicitly represented; and (iii) the amount of water available for irrigation. Following Winchester and Reilly (2015), we consider two policy cases. The reference case imposes 'business as usual' trajectories for population and GDP as specified in the data sources listed Section 2.1. It also includes renewable fuel mandates in the EU and the US, extended through the 2050 horizon of our study, but it does not include any other policies that would create incentives to expand bioenergy production. In the policy case, we add to the assumption in the reference case, a global price on all GHG emissions except those from land use change of \$25 per metric tonne of CO₂ equivalent (tCO_{2e}) in 2015 and rising by 4 per cent per year to \$99/tCO_{2e} in 2050. This was chosen because it creates greater incentives for bioenergy production, and an interest of our research of whether, under expanded demand for land resources from bioenergy, water constraints pose a more serious concern and ultimately limit bioenergy expansion.

Three alternatives for water availability are considered: constant; increasing; and decreasing. In the constant case, water available for irrigation is fixed at its 2010 level in all regions. In the decreasing case, beginning in 2015, water available for irrigation in each region decreases by 2.5 per cent relative to the 2010 level every 5 years, so water available for irrigation in 2050 is 20 per cent lower than in 2010. In the increasing case, equivalent increases are simulated, and water available for irrigation is 20 per cent higher in each region in 2050 relative to 2010. Yields on rainfed land are constant across water availability cases.⁸

These changes in water availability are illustrative and are designed to highlight sensitivities of the model to changes in water availability. Actual changes could come from greater demand for water uses and/or from changes in climate. While the former would most likely reduce water availability for irrigation, the latter could increase or decrease availability. Irrigation is responsible for about 80 per cent of current water consumption worldwide (MIT Joint Program 2014), and so a 20 per cent reduction, assuming no

⁸ The sensitivity of our results to the assumption that yields on rainfed land are constant when water available for irrigation is changed is examined in the supporting information for this paper.

change in supply would allow a doubling of all other uses. Overall, climate change is expected to speed up the hydrological cycle and increase precipitation but water availability in rivers and lakes is the result of uncertain patterns of climate change and complex interactions with temperature, land cover and evapotranspiration. While beyond the scope of this paper, the model developments reported here are designed to allow consideration of shifts in the irrigable water supply function that can be derived from the WRS. The WRS can use IGSM (Sokolov *et al.* 2005) projections of changing climate or that of other climate models.

To understand the impact of implicitly representing irrigated land, it is important to realise that in EPPA with aggregated cropland, crop production costs and yields are production-weighted averages of those on rainfed and irrigated cropland. Irrigated crops, and production from them, are included in the base data and model, but are not explicitly differentiated. The implication in that formulation is that as aggregate cropland production expands, the proportion of rainfed and irrigable land expand proportionally, and non-land costs of adding additional irrigable capacity are constant. Hence, there is no scarcity of water, no reason to invest in technology that increases efficiency, and no ultimate limit on irrigable land in such a formulation. In contrast, in our new formulation, marginal costs of expanding irrigation capacity are increasing, implicit scarcity rents exist for water used on inframarginal irrigated acres, and the proportions of rainfed and irrigable cropland can vary over time depending on the ease of expanding and the value/yields from additional production on each land type.

We expect the costs of expanding crop production to differ in the revised formulation of the model which will result in differences in macroeconomic welfare, areas devoted to crops, food prices and other metrics. The revision has two opposing effects. On the one hand, rising marginal irrigation costs means that expansion of irrigable areas is more expensive than when aggregate cropland is considered. On the other hand, freeing the model from the constraint of a constant proportion of irrigated cropland in total cropland may result in lower costs of expanding crop production. In some regions, it may be cheaper to improve irrigation systems than to use more cropland, while in others it may be cheaper to use more rainfed cropland rather than irrigating additional land. On balance, we expect rising marginal irrigation costs to result in more costly crop production when irrigated land is represented. However, the effect of relaxing the fixed proportion constraint will reduce overall impacts and can lead to reduced crop production costs in regions with low incremental irrigation costs and/or high cropland rents.

In contrast to our method representing irrigated land, the common approach in economy-wide models of using a constant elasticity of transformation (CET) function to allocate land between irrigated and rainfed uses and assuming substitutability between land and water in production imposes rigid restrictions on how crop production can expand. Specifically, under the CET approach any transition from irrigated to rainfed land is

costly; it reduces the benefit of changing the ratio of irrigated to rainfed land. Furthermore, including land and water as imperfect substitutes in production prevents water resources from being used more efficiently by using more capital and other inputs.

The scenarios are designed to address four broad questions. First, comparing results for the *Reference* policy setting with *No* water constraints explicitly represented (*Ref-N*) with the *Reference* policy setting and 100 per cent of water for irrigation available (*Ref-100%*) allows us to quantify the impact of explicitly representing irrigable cropland at current water availability. A key question is the extent and direction of bias, if any, of models that only identify aggregated cropland. A second broad question is whether results are sensitive to changes in the amount of available water, which we test in the *Reference* scenario by decreasing water availability to 80 per cent (*Ref-80%*) or increasing it to 120 per cent (*Ref-120%*) of currently available water. We are also interested in the effect of explicit water constraints on bioenergy expansion, which we can determine by comparing a *Policy* with *No* water constraints (*Pol-N*) scenario, with a *Policy* scenario with water availability at 100 per cent of our of the current level (*Pol-100%*). Here the key question is: Does explicit representation of water constraints change our estimate of commercial biomass energy supply potential (or price impacts on food) substantially when compared with the same policy stimulus for bioenergy, but no explicit water constraint? Finally, we are interested in whether less (*Pol-80%*) or more (*Pol-120%*) water availability affects our conclusions on bioenergy expansion. The details of the eight scenarios are summarised in Table 1.

4. Results

We organise results in two sections, first answering our four main questions, focusing on results in 2050. We then present some of the broad energy, bioenergy and land use results.

4.1. Economic, environment, land use and bioenergy implications of irrigation

Table 2 reports a summary of global results in 2050 with additional results in Figures 1–5. From this table, we can address the four questions we set out to answer. First, what is the extent and direction of bias, if any, of models that only identify aggregated cropland? Overall, comparing *Ref-100%* to *Ref-N* we find that including water constraints reduces global welfare (measured as the annual equivalent variation in consumer income) by 0.35 per cent, food use (total demand for food as an intermediate inputs and for final consumption) declines by 0.2 per cent and food prices rise by 0.14 per cent. Overall, these are relatively minor effects, measured at the global level. One reason for the small impacts is that irrigated area expands less than in proportion to rainfed land when flexibility is allowed. Hence, food

Table 1 Scenarios considered

Scenario	Carbon price?	Irrigated land?	Water resources
<i>Ref-N</i>	No	No	Not explicitly represented
<i>Ref-80%</i>	No	Yes	Beginning in 2015, water available for irrigation in each region decreases by 2.5% relative to the 2010 level every 5 years, so water availability in 2050 are 20% lower than in 2010
<i>Ref-100%</i>	No	Yes	Water available for irrigation is fixed at its 2010 level in all regions
<i>Ref-120%</i>	No	Yes	Beginning in 2015, water available for irrigation in each region increases by 2.5% relative to the 2010 level every 5 years, so water availability in 2050 are 20% higher than in 2010
<i>Pol-N</i>	Yes	No	Not explicitly represented
<i>Pol-80%</i>	Yes	Yes	Beginning in 2015, water available for irrigation in each region decreases by 2.5% relative to the 2010 level every 5 years, so water availability in 2050 are 20% lower than in 2010
<i>Pol-100%</i>	Yes	Yes	Water available for irrigation is fixed at its 2010 level in all regions
<i>Pol-120%</i>	Yes	Yes	Beginning in 2015, water available for irrigation in each region increases by 2.5% relative to the 2010 level every 5 years, so water availability in 2050 are 20% higher than in 2010

production expansion uses more of the less-costly rainfed land. In *Ref-N*, 1,765 Mha of land is used globally for food crops and this increases to 1,774 Mha in *Ref-100%*. Relative to the *Ref-N* scenario, global irrigated cropland decreases by 43 (346–389) Mha and rainfed cropland increases by 53 (1,428–1,375) Mha resulting in total land used for food crops increasing by 9 Mha (0.5 per cent).⁹ However, rainfed land is less productive explaining the decline in food use (and food production) and increase in food prices.

Interestingly, more bioenergy is produced when irrigated land is explicitly represented than when there is one type of cropland (i.e. primary bioenergy is 29.5 EJ in the *Ref-100%* scenario and 28.5 EJ in the *Ref-N* scenario). This change is driven by bioenergy production in India, where less land is needed for food crops in the *Ref-100%* scenario than the *Ref-N* case. This occurs because the implicit constraint that rainfed and irrigated land must be added in fixed proportions in the *Ref-N* scenario results in higher land prices relative to the *Ref-100%* scenario, where the proportion of irrigated land can change but the marginal cost of expanding irrigation is increasing.

⁹ As noted in Section 3, when irrigated land is not explicitly represented, the model implicitly assumes that irrigable land is a fixed proportion of total crop land. We exploit this assumption to calculate changes in irrigable crop land in scenarios that do not explicitly represent this type of land.

Table 2 Summary of global results in 2050

	Ref-N	Ref-80%	Ref-100%	Ref-120%	Pol-N	Pol-80%	Pol-100%	Pol-120%
Welfare change (%)		-0.35	-0.35	-0.35	-3.18	-3.59	-3.60	-3.61
CO ₂ e emissions (MMt)	74,145	73,801	73,814	73,771	42,741	41,306	41,136	41,332
Primary energy (EJ)	699.8	703.1	703.0	703.1	516.6	517.6	517.8	517.8
Primary bioenergy (EJ)	28.5	29.4	29.5	29.7	140.9	142.5	142.7	142.8
Final bioenergy (EJ)	14.5	15.1	15.2	15.3	67.3	68.3	68.49	68.51
Bioenergy land (Mha)	13.5	12.9	13.1	13.3	152.2	150.1	150.53	150.64
Food cropland (Mha)	1,765	1,769	1,774	1,778	1,646	1,649	1,653	1,656
Rainfed land (Mha)	1,375	1,444	1,428	1,427	1,271	1,335	1,320	1,320
Irrigated land (Mha)	389	325	346	351	375	315	333	337
Natural Forest land (Mha)	3,993	3,997	3,997	3,997	3,818	3,827	3,826	3,826
Managed grassland (Mha)	3,064	3,064	3,060	3,057	3,196	3,193	3,191	3,188
Change in food use (%)	—	-0.26	-0.2	-0.18	-4.1	-4.48	-4.47	-4.47
Change in food price (%)	—	0.23	0.14	0.12	3.73	4.10	4.05	4.03

Notes: Scenarios are differentiated by the existence of a carbon price (Ref or Pol) and the availability of water in 2050 relative to in 2010 (80%, 100%, 120%, or N, not explicitly represented). Per cent changes are relative to the *Ref-N* scenario.

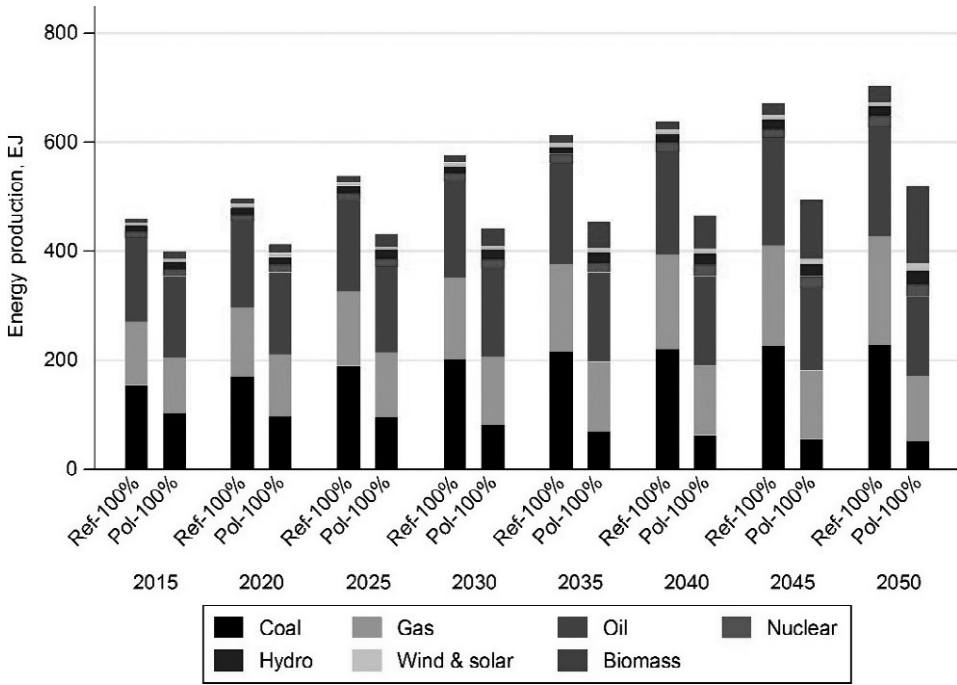


Figure 1 Global primary energy through 2050. Scenarios are differentiated by the existence of a carbon price (Ref or Pol) and the availability of water in 2050 relative to the level in 2010 (80 per cent, 100 per cent, 120 per cent or *N*, not explicitly represented).

A further interesting result is that explicitly representing irrigated land increases natural forest areas relative to when a single cropland type is included. For example, natural forest cover is 3,997 Mha in the *Ref-100%* scenario and 3,993 Mha in the *Ref-N* scenario. While a small difference, it is in the reverse direction one might expect. It is due to a shift in livestock production from regions with more land-intensive livestock production (Africa and China) to regions with less land-intensive production (the EU, the US and India), which reduces global managed grassland and provides scope for less deforestation (and more natural forest) in Africa and China. More natural forest land when irrigated land is explicitly represented also results in less CO₂e emissions than in the *Ref-100%* scenario relative to the *Ref-N* case.

Moving to our second question: Are results sensitive to changes in the amount of available water? Comparing *Ref-80%* and *Ref-120%* to *Ref-100%*, we see results that are generally in the direction one would expect. Less water increases the welfare loss, results in higher food prices, less food consumption and less irrigated land compared to *Ref-100%*, and *vice versa* when there is more water. Increasing water availability leads to more land devoted to bioenergy and more bioenergy production, but changes are small (e.g. global primary bioenergy increases from 29.4 EJ in *Ref-80%* to 29.7 EJ in *Ref-120%*). Total food cropland is less when there is less water and more

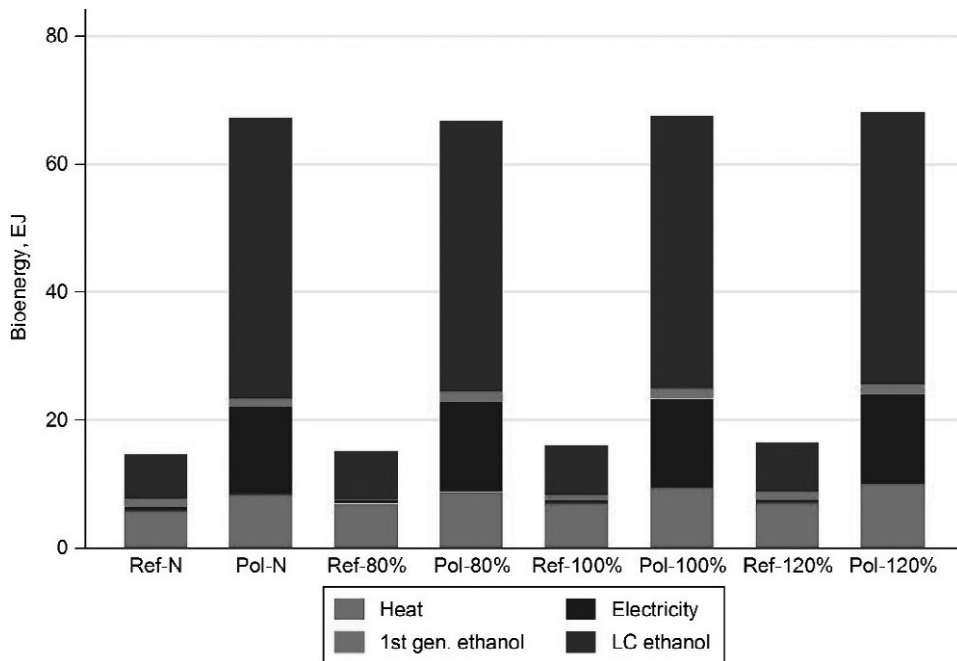


Figure 2 Global final bioenergy in 2050. Scenarios are differentiated by the existence of a carbon price (Ref or Pol) and the availability of water in 2050 relative to the level in 2010 (80 per cent, 100 per cent, 120 per cent or *N*, not explicitly represented).

when there is more water. While there is a switch towards rainfed from irrigated cropland in all scenarios with irrigated land explicitly modelled, comparing *Ref-80%* to *Ref-100%*, land expansion is overall more expensive. The flexibility to use rainfed instead of irrigated land exists in both of these scenarios, unlike the comparison of *Ref-N* and *Ref-100%* where the new flexibility of expanding irrigated and rainfed land in different proportions had a partially offsetting effect on food prices (and hence land area). Again, while these results are generally in the direction we expect, the magnitudes of global changes are small especially looking at the food price effects, which remain well below 1 per cent even with less water.

Regarding our third question: Does explicit representation of water resources change our estimate of commercial biomass energy supply potential and its effects on the economy and environment? The comparison of *Pol-N* and *Ref-N* was the basis of an earlier paper (Winchester and Reilly 2015) and the policy impacts shown here are similar, with the differences resulting from the revised cost estimates for LC ethanol used in this study. In that paper, the food price impacts were decomposed into those due to expansion of bioenergy and those due to higher energy prices and other impacts of the overall GHG pricing policy. The paper found that about 60 per cent of the increase in food prices was due to the carbon price increasing costs throughout the economy, and around 40 per cent were due to the production

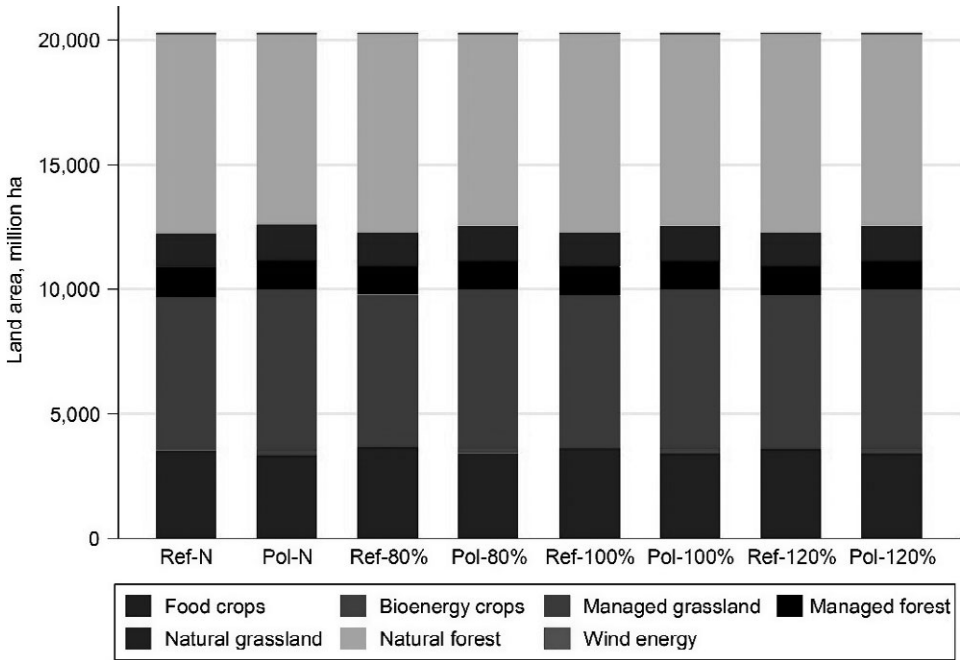


Figure 3 Global land use in 2050. Scenarios are differentiated by the existence of a carbon price (Ref or Pol) and the availability of water in 2050 relative to the level in 2010 (80 per cent, 100 per cent, 120 per cent, or *N*, not explicitly represented).

of bioenergy.¹⁰ The relatively small impacts of a significant (*c.* 150 EJ) commercial bioenergy industry on food prices led to the question of whether a lack of water constraints in that version of the model led to a serious underestimate of the impacts and/or the ability to expand bioenergy. Comparing *Pol-100%* and *Pol-N* quantitatively answers that question. As hypothesised, water constraints increase the overall cost of the policy by about 13 per cent or 0.42 percentage points (3.60–3.18 per cent). While the 0.42 percentage point increase is small, that this one additional feature increases the overall climate policy cost on order of 15 per cent is not insubstantial. The food price increases in the *Pol-100%* scenario (4.05 per cent) is greater than in *Pol-N* scenario (3.73 per cent) but it remains relatively small, at least compared with concerns in the 2007–2008 period where some authors (e.g. Mitchell 2008) attributed a significant portion of the spike in crop and food prices at the time to biofuel expansion (at much lower levels). Explicitly representing irrigable land increases natural forest areas (by reducing the rate of deforestation) and increases bioenergy production (by a small amount) through the same indirect routes earlier described for the *Ref* cases.

¹⁰ The drivers of the increase in food price are decomposed by simulating each scenario without any bioenergy pathways and comparing the changes in food prices to those in the core scenarios (with bioenergy technologies).

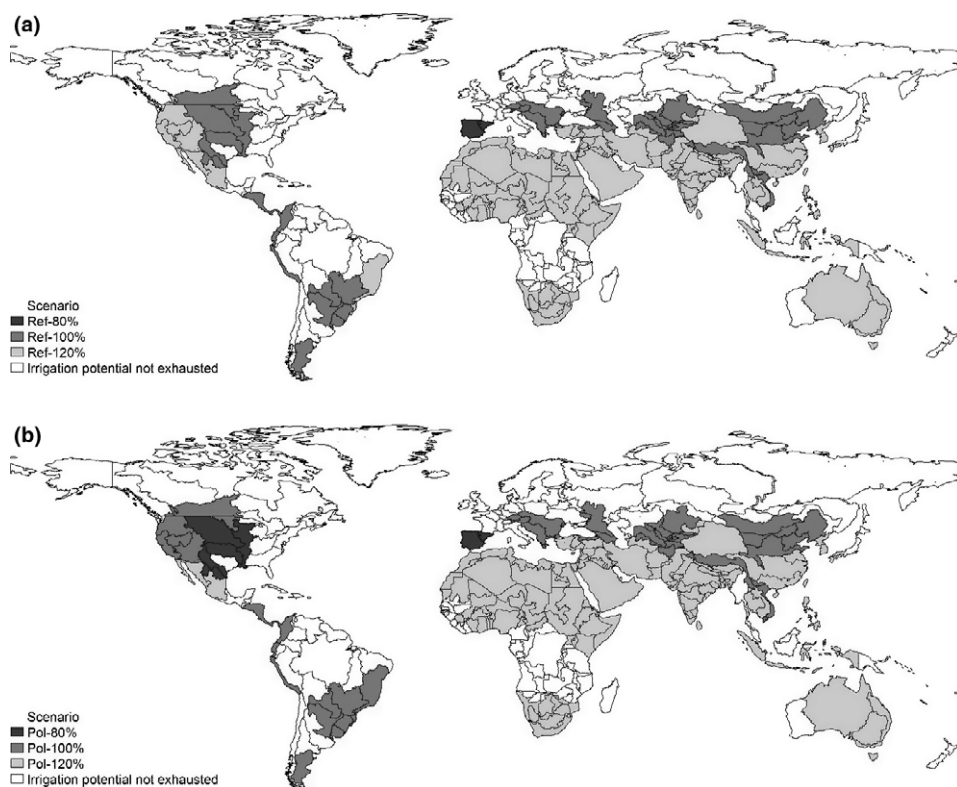


Figure 4 Food producing units (FPUs) operating at maximum irrigation potential in the (a) Reference and (b) Policy cases in 2050. Scenarios are differentiated by the existence of a carbon price (Ref or Pol) and the availability of water in 2050 relative to the level in 2010 (80 per cent, 100 per cent, 120 per cent or *N*, not explicitly represented).

Moving to our fourth question: Does less or more water availability affect our conclusions on bioenergy expansion and its effects on the economy and environment? Comparing *Pol-100%* and *Pol-80%* reveals results in the expected direction – higher welfare costs, higher food prices, less food used and less bioenergy – but the differences are quite small. The welfare cost increase is 0.01 percentage points (a 0.3 per cent increase in welfare cost), and the food price impact of 0.05 percentage points increases the food price impact by 1.2 per cent. Primary bioenergy production is reduced from 142.7 to 142.5 EJ (0.14 per cent).

4.2 Energy, bioenergy and land use results

The GHG pricing policy is implemented gradually, assumed to have started in 2015 at \$25 and rising to \$99/tonne CO₂e by 2050. This policy initially reduces global energy use by about 50 EJ, and the rising CO₂e price keeps energy use well below the *Ref-100%* scenario (Figure 1). Important for climate concerns, fossil energy use continues to drift down through 2050 with

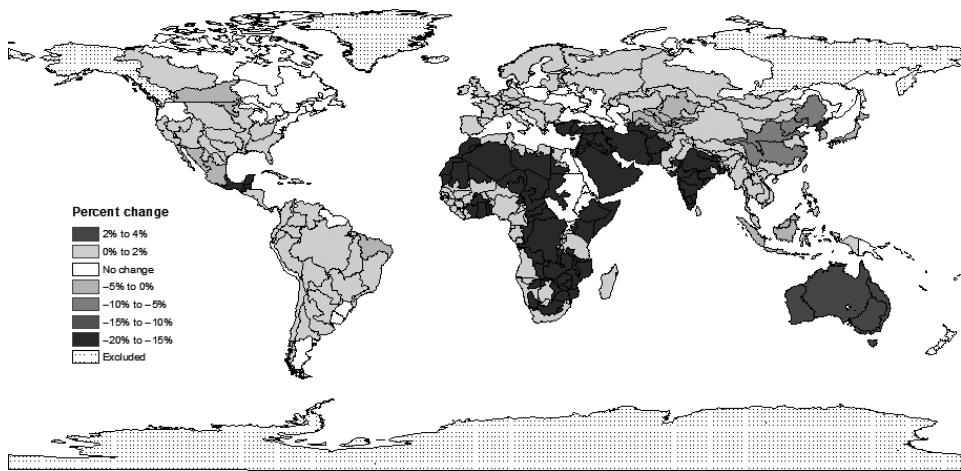


Figure 5 Proportional changes in irrigable land in 2050 by food producing units (FPU) in the Reference scenario with 80 per cent of current water resources available (*Ref-80%*) relative to the Reference scenario with 100 per cent of current water resources available (*Ref-100%*).

Note: The 'rest of the world' water region defined by Rosegrant *et al.* (2012) includes 'residual' river basins in several areas. Due to data limitations for this water region, changes in irrigated land in these river basins (shaded with dots) are not reported in the figure.

coal use dropping substantially. While other low carbon sources of energy expand, the main reason energy use is able to increase, while fossil energy decreases, is because of the substantial contribution from bioenergy.

The biggest increase in bioenergy by 2050 as a result of the policy is from ethanol produced via a LC production pathway (Figure 2). Given the assumed cost reductions in LC-ethanol, it becomes generally less expensive than corn-based ethanol, especially with the carbon price that penalises corn-based ethanol because it uses fossil fuels that emit GHGs. There remains some first-generation ethanol, primarily sugarcane-based from Brazil. There is also a large increase in bioenergy used for electricity, from almost none in the *Ref* scenarios to about 15 EJ in the policy scenarios. Bioenergy used for heat contributes about 5 EJ in the *Ref* scenarios. It slightly increases in the *Pol* scenarios. Other bioenergy forms and production pathways are not commercially viable in 2050 given these economic and policy scenarios. As previously noted, the explicit representation of irrigable land and sensitivity to available water (± 20 per cent) has very small overall impacts, barely detectable in Figures 1 and 2, and are not reported in this sub-section.

There are slight differences in land area in different land use types, mostly in comparing *Ref* and *Pol* scenarios (Figure 3). The differences between scenarios with or without irrigated land explicitly modelled are, again, so small as to be barely detectable in a figure plotting total land areas. Similar to Winchester and Reilly (2015) the land needed for bioenergy is quite small compared with other land uses.¹¹ There are a number of reasons: the energy

¹¹ The impacts of bioenergy on land use and other outcomes are consistent with optimistic projections for the global potential of bioenergy reviewed by Berndes *et al.* (2003).

yield of woody and grassy crops per hectare is fairly high, agricultural and forest waste provides some of the biomass feedstock, and we include a gradual improvement in yields over time. With the small land impacts, it is not surprising that the food price impacts are also small.

While water constraints are not a problem globally, some water regions are using all of the irrigable lands we estimated to be available to them (Figure 4). Yellow regions are at their maximum irrigation potential (i.e. when conveyance and irrigation systems operate at maximum efficiency and storage is such that annual water yield is equal to average runoff) even with water availability at 120 per cent of what we estimate is currently available. Orange regions are also at their maximum, at 100 per cent of currently available water, and red regions hit the maximum potential if water availability drops to 80 per cent of that currently available. Maximum irrigation capacity is predicted to be exhausted in many regions with rapidly growing populations and/or arid climates. Comparing Figures 4a and b indicates that bioenergy production has a small impact on the number of FPU's operating at maximum irrigating potential, which is consistent with bioenergy accounting for a small proportion of total cropland. The implication is that water shortage and stress is a significant concern in many regions, there is likely to be considerable pressure (and value) to improve efficiency of water use and conveyance, and to add additional storage wherever possible in many parts of the world. If those adaptations in the water system are made, and trade in agricultural products (and biomass crops) is an option then these regional water shortfalls need not impinge on the ability to produce bioenergy.

Proportional changes in irrigable land in 2050 by FPU in the *Ref-80%* scenario relative to the *Ref-100%* scenario are displayed in Figure 5. This figure further highlights that small changes at the global level mask large impacts in some regions. The decrease in water resources has the largest impacts on irrigable land in FPU's in Africa, China, India, Mexico and the Middle East; regions that have high costs of irrigation expansion. In several other FPU's, there are small increases in irrigable land. These results support Liu *et al.*'s (2014) finding that international agricultural trade mitigates the local impacts of changes in water availability.

5. Conclusions

Feeding a growing global population and promoting bioenergy to mitigate climate change will put pressure on food prices and land markets. Land use responses to the increased demand for biomass will depend on constraints on the expansion of irrigated land. If expanding irrigation is expensive or limited, deforestation may be needed to bring more rainfed land into crop production to meet food demand, and bioenergy production will be more costly and could be curtailed.

This paper advances the understanding of food, bioenergy, water and land outcomes by representing irrigated land supply curves in the MIT EPPA model. The irrigable land supply curves were based on spatial-level estimates of the costs of improving irrigation efficiency and increasing water storage, and facilitate the representation of endogenous changes in irrigation infrastructure. The model was simulated under a global carbon price with the objective of determining how food, bioenergy and deforestation are affected: (i) when irrigated land is explicitly represented, relative to when only a single type of cropland is considered; and (ii) by changes in water availability.

We found that explicitly representing irrigated land had small impacts on global modelling outcomes relative to when only a single type of cropland is included. This is primarily because representing a single cropland type implicitly assumes that irrigated and rainfed land must expand in equal proportions. When irrigated and rainfed land are separately identified, although rising marginal costs for expanding irrigable land make increasing the quantity of irrigated land more expensive, allowing greater flexibility by relaxing the equal-proportion assumption can decrease the cost of expanding crop production. This representation allowed more flexibility than previous approaches to including irrigated land in economy-wide models.

We also found that changing water availability for agriculture by plus or minus 20 per cent had small global impacts on food prices, bioenergy production and deforestation. This is because, unlike in the traditional CET approach to including irrigated land in economy-wide models, 1 ha of land released from irrigated production can be used in rainfed production. The impacts of changes in water availability on food, bioenergy and land use were also mitigated in our model by endogenous improvements in irrigation efficiency and water storage, which allowed additional water to be ‘produced’ using capital, labour and other inputs. Despite the small global impacts, we observed that irrigation outcomes were very sensitive to water availability in some regions.

Another interesting result was that heterogeneity in irrigation production and expansion possibilities can drive shifts in the global composition of livestock production. In our simulations, livestock production relocated from regions with more land-intensive production to regions with less land-intensive production. As global pasture land is three times the size of global cropland, these land-saving changes increased natural forest areas, even when there was increased demand for cropland.

We close with cautionary notes on our methods and the design of our experiments. First, as we augmented a global model, the spatial resolution of some irrigation cost estimates is coarse relative to the local nature of some water issues. In this connection, Ledvina *et al.* (2017) provide tools that allow users to modify the data and parameters used to estimate the irrigable land supply curves. Second, our analysis examined a specific shock that changed the quantity of water available for irrigation (due to a change in demand for

other uses) under constant climate conditions. As such, there were no direct impacts on crop yields on either rainfed or irrigated land. In the future, temperature and precipitation changes will not only directly impact yields, but also water availability through runoff and evaporation. Addressing outcomes under climate change requires an integrated analysis. While such an assessment is beyond the scope of this study, the EPPA model forms part of the MIT IGSM, and the extended model developed in the paper could be included in an integrated analysis in future work.

References

- Aguiar, A., Narayanan, B. and McDougall, R. (2016). An overview of the GTAP 9 data base, *Journal of Global Economic Analysis* 1, 181–208.
- Armington, P.S. (1969). A theory of demand for products distinguished by place of production, *IMF Staff Papers* 16, 159–176.
- Baker, J. (2011). The impact of including water constraints on food production within a CGE framework. Master of Science Thesis, Massachusetts Institute of Technology. Available from URL: http://globalchange.mit.edu/files/document/Baker_MS_2011.pdf [accessed 20 March 2018].
- Berndes, G., Hoogwijk, M. and van den Broek, R. (2003). The contribution of biomass in the future global energy supply: a review of 17 studies, *Biomass Bioenergy* 25, 1–28.
- Berrittella, M., Hoekstra, A., Rehdanz, K., Roson, R. and Tol, R. (2007). The economic impact of restricted water supply: a computable general equilibrium analysis, *Water Research* 41, 1,799–1,813.
- BP (2015). *BP Technology Outlook*. London, UK. Available from URL: <http://www.bp.com/content/dam/bp/pdf/technology/bp-technology-outlook.pdf> [accessed Nov 2015].
- Calzadilla, A., Rehdanz, K. and Tol, R. (2010). The economic impact of more sustainable water use in agriculture: a computable general equilibrium analysis, *Journal of Hydrology* 384, 292–305.
- Dinar, A. (2014). Water and economy-wide policy interventions, *Foundations and Trends in Microeconomics* 10, 85–163.
- Gurgel, A., Reilly, J.M. and Paltsev, S. (2007). Potential land use implications of a global biofuels industry, *Journal of Agricultural & Food Industrial Organization* 5, 1–34.
- Gurgel, A., Cronin, T., Reilly, J.M., Paltsev, S., Kicklighter, D. and Melillo, J. (2011). Food, fuel, forests and the pricing of ecosystem services, *American Journal of Agricultural Economics* 93, 342–348.
- Haqiqi, I., Taheripour, F., Liu, J. and van der Mensbrugge, D. (2016). Introducing irrigation water into GTAP data base version 9, *Journal of Global Economic Analysis* 1, 116–155.
- International Energy Agency (IEA) (2006). *World Energy Outlook: 2007*. OECD/IEA, Paris. Available from URL: <https://www.iea.org/publications/freepublications/publication/wo2006.pdf> [accessed 20 March 2018].
- International Energy Agency (IEA) (2012). *World Energy Outlook: 2007*. OECD/IEA, Paris. Available from URL: <http://www.worldenergyoutlook.org/publications/weo-2012> [accessed 20 March 2018].
- International Monetary Fund (IMF) (2013). *World Economic Outlook*. International Monetary Fund. Available from URL: <http://www.imf.org/external/pubs/ft/weo/2013/01/weodata/download.aspx> [accessed 20 March 2018].
- Ledvina, K., Winchester, N., Strzepek, K. and Reilly, J.M. (2017). New data for representing irrigated agriculture in economy-wide models. MIT JPSPGC Report 321, October, 16 pp. Available from URL: https://globalchange.mit.edu/sites/default/files/MITJPSPGC_Rpt321.pdf [accessed 20 March 2018].

- Liu, J., Hertel, T.W., Taheripour, F., Zhu, T. and Ringler, C. (2014). International trade buffers the impact of future irrigation shortfalls, *Global Environmental Change* 29, 22–31.
- Melillo, J.M., Reilly, J.M., Kicklighter, D.W., Gurgel, A.C., Cronin, T.W., Paltsev, S., Felzer, B.S., Wand, X., Sololov, A.P. and Schlosser, C.A. (2009). Indirect emissions from biofuels: how important?, *Science* 326, 1,397–1,399.
- MIT Joint Program (2014). *2014 Climate and Energy Outlook*. MIT Joint Program on the Science and Policy of Global Change, Cambridge, MA. Available from URL: <https://globalchange.mit.edu/sites/default/files/newsletters/files/2014%20Energy%20%26%20Climate%20Outlook.pdf> [accessed 20 March 2018].
- Mitchell, D. (2008). A note on rising food prices. The World Bank, Development Prospects Group, Policy Research Working Paper No. 4682, July, 21 pp. Available from URL: http://www-wds.worldbank.org/external/default/WDSContentServer/WDSP/IB/2008/07/28/000020439_20080728103002/Rendered/PDF/WP4682.pdf [accessed 20 March 2018].
- Narayanan, B.G. and Walmsley, T.L. (Eds.). (2008). *Global Trade, Assistance, and Production: The GTAP 7 Data Base*. Center for Global Trade Analysis, Purdue University, West Lafayette, Indiana.
- Paltsev, S., Reilly, J., Jacoby, H.D., Eckaus, R.S., McFarland, J., Sarofim, M., Asadoorian, M. and Babiker, M. (2005). The MIT Emissions Prediction and Policy Analysis (EPPA) model: version 4. MIT JPSPGC Report 125, August, 78 pp. Available from URL: http://globalchange.mit.edu/files/document/MITJPSPGC_Rpt125.pdf [accessed 20 March 2018].
- Portmann, F.T., Siebert, S. and Döll, P. (2010). MIRCA2000 Global monthly irrigated and rainfed crop areas around the year 2000: a new high-resolution data set for agricultural and hydrological modeling, *Global Biogeochemical Cycles*, 24, 1–24.
- Rosegrant, M.W., Ringler, C., Msangi, S., Sulser, T.B., Zhu, T. and Cline, S.A. (2012). *International Model for Policy Analysis of Agricultural Commodities and Trade (IMPACT) Model Description*. International Food Policy Research Institute. Available from URL: <http://technicalconsortium.org/wp-content/uploads/2014/05/International-model-for-policy-analysis.pdf> [accessed 20 March 2018].
- Rutherford, T.F. (1995). Extension of GAMS for complementary problems arising in applied economic analysis, *Journal of Economic Dynamics and Control* 19, 1,299–1,324.
- Rutherford, T.F. (2002). *Lecture Notes on Constant Elasticity Functions*. University of Colorado. Available from URL: <http://www.gamsworld.org/mpsge/debreu/ces.pdf> [accessed 20 March 2018].
- Siebert, S. and Döll, P. (2010). Quantifying blue and green virtual water contents in global crop production as well as potential production losses without irrigation, *Journal of Hydrology* 384, 199–217.
- Sokolov, A.P., Schlosser, C.A., Dutkiewicz, S., Paltsev, S., Kicklighter, D.W., Jacoby, H.D., Prinn, R.G., Forest, C.E., Reilly, J.M., Wang, C., Felzer, B., Sarofim, M.C., Scott, J., Stone, P.H., Melillo, J.M. and Cohen, J. (2005). The MIT Integrated Global System Model (IGSM) Version 2: model description and baseline evaluation, MIT JPSPGC Report 124, July 40 pp. Available from URL: http://web.mit.edu/globalchange/www/MITJPSPGC_Rpt124.pdf [accessed 20 March 2018].
- Strzepek, K., Schlosser, C.A., Gueneau, A., Gao, X., Blanc, E., Fant, C., Rasheed, B. and Jacoby, H.D. (2013). Modeling water resource systems within the framework of the MIT Integrated Global System Model: IGSM-WRS, *Journal of Advances in Modeling Earth Systems* 5, 638–653.
- Taheripour, F., Zhuang, Q., Tyner, W.E. and Lu, X. (2012). Biofuels, cropland expansion, and the extensive margin, *Energy, Sustainability and Society* 2, 25.
- Taheripour, F., Hertel, T.W. and Liu, J. (2013a). Introducing water by river basin into the GTAP-BIO model: GTAP-BIO-W. GTAP Working paper No. 77. Available from URL: <https://www.gtap.agecon.purdue.edu/resources/download/6648.pdf> [accessed March 20 2018].

- Taheripour, F., Hertel, T.W. and Liu, J. (2013b). The role of irrigation in determining the global land use impacts of biofuels, *Energy Sustainability and Society* 3, 1–18.
- United Nations (UN) (2011). *World Population Prospects: The 2010 Revision*. Population Division, United Nations Department of Economic and Social Affairs, New York City, New York.
- van Tongeren, F., Koopman, R., Karingi, S., Reilly, J. and Francois, J. (2017). Back to the future: a 25-year retrospective on GTAP and the shaping of a new agenda, *Journal of Global Economic Analysis* 2, 1–42.
- Wiberg, D.A. and Strzepek, K. (2005). Development of regional economic supply curves for surface water resources and climate change assessment: a case study of China. The International Institute for Applied Systems Analysis, Research Report 05-001, Vienna, Austria.
- Winchester, N. and Reilly, J.M. (2015). The feasibility, costs, and environmental implications of large-scale biomass energy, *Energy Economics* 51, 188–203.

Supporting Information

Additional Supporting Information may be found in the online version of this article:

Data S1. Results when yields on rainfed cropland are positively correlated with water availability.

Figure S1. Rainfed and irrigated harvested area by EPPA region.

Figure S2. The value of crop production on rainfed and irrigated areas by EPPA region.

Figure S3. Food producing units (outlines) and water regions (color groupings).

Figure S4. Annual irrigable land supply curve for the Mississippi River water region.

Figure S5. Irrigation response units (distinguished by color) for India built on clustered water regions.

Figure S6. Irrigated crop production in an IRU in the EPPA model.

Figure S7. Production of irrigated land permits for each IRU in the EPPA model.

Table S1. Aggregation in the EPPA model extended to represent bioenergy in detail.

Table S2. Water regions included in each EPPA region.

Table S3. Irrigation and scheme efficiency with and without canal lining.

Table S4. The mapping of water regions to IRUs.

Table S5. Summary of global results in 2050 when yields on rainfed cropland are positively correlated with water availability.

Joint Program Reprint Series - Recent Articles

For limited quantities, Joint Program publications are available free of charge. Contact the Joint Program office to order.

Complete list: <http://globalchange.mit.edu/publications>

2018-3 The Impact of Water Scarcity on Food, Bioenergy and Deforestation. Winchester, N., K. Ledvina, K. Strzepek and J.M. Reilly, *Australian Journal of Agricultural and Resource Economics*, online first (doi:10.1111/1467-8489.12257) (2018)

2018-2 Modelling Ocean Colour Derived Chlorophyll-a. Dutkiewicz, S., A.E. Hickman and O. Jahn, *Biogeosciences* 15: 613–630 (2018)

2018-1 Hedging Strategies: Electricity Investment Decisions under Policy Uncertainty. Morris, J., V. Srikrishnan, M. Webster and J. Reilly, *Energy Journal*, 39(1) (2018)

2017-24 Towards a Political Economy Framework for Wind Power: Does China Break the Mould?. Karplus, V.J., M. Davidson and F. Kahrl, Chapter 13 in: *The Political Economy of Clean Energy Transitions*, D. Arent, C. Arent, M. Miller, F. Tarp, O. Zinaman (eds.), UNU-WIDER/Oxford University Press, Helsinki, Finland (2017)

2017-23 Carbon Pricing under Political Constraints: Insights for Accelerating Clean Energy Transitions. Karplus, V.J. and J. Jenkins, Chapter 3 in: *The Political Economy of Clean Energy Transitions*, D. Arent, C. Arent, M. Miller, F. Tarp, O. Zinaman (eds.), UNU-WIDER/Oxford University Press, Helsinki, Finland (2017)

2017-22 “Climate response functions” for the Arctic Ocean: a proposed coordinated modelling experiment. Marshall, J., J. Scott and A. Proshutinsky, *Geoscientific Model Development* 10: 2833–2848 (2017)

2017-21 Aggregation of gridded emulated rainfed crop yield projections at the national or regional level. Blanc, É., *Journal of Global Economic Analysis* 2(2): 112–127 (2017)

2017-20 Historical greenhouse gas concentrations for climate modelling (CMIP6). Meinshausen, M., E. Vogel, A. Nauels, K. Lorbacher, N. Meinshausen, D. Etheridge, P. Fraser, S.A. Montzka, P. Rayner, C. Trudinger, P. Krümmel, U. Beyerle, J.G. Cannadell, J.S. Daniel, I. Enting, R.M. Law, S. O’Doherty, R.G. Prinn, S. Reimann, M. Rubino, G.J.M. Velders, M.K. Vollmer, and R. Weiss, *Geoscientific Model Development* 10: 2057–2116 (2017)

2017-19 The Future of Coal in China. Zhang, X., N. Winchester and X. Zhang, *Energy Policy*, 110: 644–652 (2017)

2017-18 Developing a Consistent Database for Regional Geologic CO₂ Storage Capacity Worldwide. Kearns, J., G. Teletzke, J. Palmer, H. Thomann, H. Kheshgi, H. Chen, S. Paltsev and H. Herzog, *Energy Procedia*, 114: 4697–4709 (2017)

2017-17 An aerosol activation metamodel of v1.2.0 of the pyrcel cloud parcel model: development and offline assessment for use in an aerosol–climate model. Rothenberg, D. and C. Wang, *Geoscientific Model Development*, 10: 1817–1833 (2017)

2017-16 Role of atmospheric oxidation in recent methane growth. Rigby, M., S.A. Montzka, R.G. Prinn, J.W.C. White, D. Young, S. O’Doherty, M. Lunt, A.L. Ganesan, A. Manning, P. Simmonds, P.K. Salameh, C.M. Harth, J. Mühle, R.F. Weiss, P.J. Fraser, L.P. Steele, P.B. Krümmel, A. McCulloch and S. Park, *Proceedings of the National Academy of Sciences*, 114(21): 5373–5377 (2017)

2017-15 A revival of Indian summer monsoon rainfall since 2002. Jin, Q. and C. Wang, *Nature Climate Change*, 7: 587–594 (2017)

2017-14 A Review of and Perspectives on Global Change Modeling for Northern Eurasia. Monier, E., D. Kicklighter, A. Sokolov, Q. Zhuang, I. Sokolik, R. Lawford, M. Kappas, S. Paltsev and P. Groisman, *Environmental Research Letters*, 12(8): 083001 (2017)

2017-13 Is Current Irrigation Sustainable in the United States? An Integrated Assessment of Climate Change Impact on Water Resources and Irrigated Crop Yields. Blanc, É., J. Caron, C. Fant and E. Monier, *Earth’s Future*, 5(8): 877–892 (2017)

2017-12 Assessing climate change impacts, benefits of mitigation, and uncertainties on major global forest regions under multiple socioeconomic and emissions scenarios. Kim, J.B., E. Monier, B. Sohngen, G.S. Pitts, R. Drapek, J. McFarland, S. Ohrel and J. Cole, *Environmental Research Letters*, 12(4): 045001 (2017)

2017-11 Climate model uncertainty in impact assessments for agriculture: A multi-ensemble case study on maize in sub-Saharan Africa. Dale, A., C. Fant, K. Strzepek, M. Lickley and S. Solomon, *Earth’s Future* 5(3): 337–353 (2017)

2017-10 The Calibration and Performance of a Non-homothetic CDE Demand System for CGE Models. Chen, Y.-H.H., *Journal of Global Economic Analysis* 2(1): 166–214 (2017)

2017-9 Impact of Canopy Representations on Regional Modeling of Evapotranspiration using the WRF-ACASA Coupled Model. Xu, L., R.D. Pyles, K.T. Paw U, R.L. Snyder, E. Monier, M. Falk and S.H. Chen, *Agricultural and Forest Meteorology*, 247: 79–92 (2017)

2017-8 The economic viability of Gas-to-Liquids technology and the crude oil-natural gas price relationship. Ramberg, D.J., Y.-H.H. Chen, S. Paltsev and J.E. Parsons, *Energy Economics*, 63: 13–21 (2017)

2017-7 The Impact of Oil Prices on Bioenergy, Emissions and Land Use. Winchester, N. and K. Ledvina, *Energy Economics*, 65(2017): 219–227 (2017)

2017-6 The impact of coordinated policies on air pollution emissions from road transportation in China. Kishimoto, P.N., V.J. Karplus, M. Zhong, E. Saikawa, X. Zhang and X. Zhang, *Transportation Research Part D*, 54(2017): 30–49 (2017)